Laboratory of Nuclear Studies, Cornell University

August 8, 2001 CBN 01-14

AN EXPLICIT FORMULA FOR UNDULATOR RADIATION

Lewis Kotredes,† Worcester Polytechnic Institute, Worcester MA 01609
and
Richard Talman, Laboratory of Nuclear Studies, Cornell University, Ithaca NY 14853

ABSTRACT

The frequency spectrum and angular distribution of radiation from an undulator is expressible as an integral over the longitudinal field profile of the undulator. In this paper this integral is approximated explicitly in terms of special functions, and the result compared with the value of the "exact" integral evaluated numerically. The agreement is excellent throughout regions of practical importance for arbitrary undulator strength K and harmonic number n. A quite complicated monochromatized angular beam profile (centered on $n = 7$ and running beyond the $n = 10$ ring) shows excellent agreement with a published (ESRF) profile.

† REU project participant, Cornell, 2001

1. Formulation of the Problem

The fundamental parameters characterizing an undulator (or wiggler) are K, where $\Theta = K/\gamma$ is the maximum angle of an electron passing through the device, the wiggler period λ_w, the number of wiggler periods N_w, and the relativistic factor γ of the electron beam. Since this paper assumes ideal electron beams, the spreads of beam direction and energy are taken to be negligibly small.

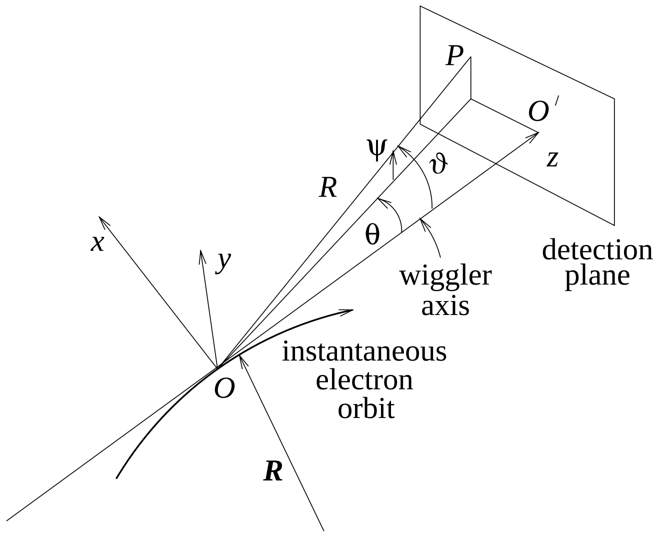

Figure 1.1: Orbit geometry and definition of horizontal angle θ and vertical angle ψ locating the detector position P relative to the wiggler axis. The orbit curvature is much exaggerated as (in the approximation of the paper) the transverse displacement (though not velocity) of the electron is neglected.

The fundamental formula to be evaluated gives the Fourier transform (frequency ω) of the electric field as observed, at observation point P in Fig. 1.1, due to a single electron of charge q passing through the undulator;[1−3]

$$\frac{\widetilde{\mathbf{E}}\left(\omega;\theta,\psi\right)}{\frac{q}{4\pi\epsilon_0 c\mathcal{R}}} = \frac{i\omega}{\sqrt{2\pi}} \int_{-\frac{N_w}{2}\frac{\lambda_w}{c}}^{\frac{N_w}{2}\frac{\lambda_w}{c}} e^{i\omega t(t_r)}\,\frac{\mathbf{v}_\perp}{c}\,dt_r\ . \tag{1.1}$$

In this formula $\mathbf{v}_\perp$ is the electron velocity normal to the line running from electon position to point P, and t is "observer time". To adequate accuracy the "retarded time" t_r is given by $z = ct_r$ where z is the electron's longitudinal position at time t_r. The (differential) relation between t and t_r is

$$\frac{dt}{dt_r} = 1 - \widehat{\mathcal{R}} \cdot \frac{\mathbf{v}\left(t_r\right)}{c}\ . \tag{1.2}$$

Approximating the orbit by a pure sinusoid, the velocity is given by

$$\frac{\mathbf{v}}{c} = \frac{v}{c}\Theta\,\cos k_w z\,\hat{\mathbf{x}} + \left(1 - \frac{1}{2\gamma^2} - \frac{\Theta^2}{2}\cos^2 k_w z\right)\hat{\mathbf{z}}, \tag{1.3}$$

where $k_w = 2\pi/\lambda_w$. Some geometric approximations to be used are

$$\begin{aligned}
&\widehat{\mathcal{R}} \approx \theta\hat{\mathbf{x}} + \psi\hat{\mathbf{y}} + \left(1 - \frac{\vartheta^2}{2}\right)\hat{\mathbf{z}}, \\
&1 - \widehat{\mathcal{R}}\cdot\frac{\mathbf{v}}{c} \approx -\theta\Theta\,\cos k_w z + \frac{1}{2\gamma^2} + \frac{\vartheta^2}{2} + \frac{\Theta^2}{2}\cos^2 k_w z, \\
&\frac{\mathbf{v}_\perp}{c} = \frac{\mathbf{v}}{c} - \left(\widehat{\mathcal{R}}\cdot\frac{\mathbf{v}}{c}\right)\widehat{\mathcal{R}} \approx (\Theta\,\cos k_w z - \theta)\,\hat{\mathbf{x}} - \psi\,\hat{\mathbf{y}} + \left(-\theta\Theta\,\cos k_w z + \vartheta^2\right)\hat{\mathbf{z}}\ .
\end{aligned} \tag{1.4}$$

where $\vartheta^2 = \theta^2 + \psi^2$. Substituting into Eq. (1.2) yields

$$\frac{d\,(ct)}{dz} = -\theta\Theta\,\cos k_w z + \frac{1 + K^2/2}{2\gamma^2} + \frac{\vartheta^2}{2} + \frac{\Theta^2}{4}\cos 2k_w z\ . \tag{1.5}$$

Integrating this equation gives the observer time t in terms of electron position z;

$$ct = \frac{1}{2\gamma^2}\left(1 + \frac{K^2}{2} + \gamma^2\vartheta^2\right)z - \frac{\theta\Theta}{k_w}\sin k_w z + \frac{\Theta^2}{8k_w}\sin 2k_w z\ , \tag{1.6}$$

This establishes the exponent in Eq. (1.1). The integrand, dropping the z-component because it is of order $1/\gamma^2$†, is

$$\frac{\mathbf{v}_\perp}{c} = \begin{pmatrix} \Theta\,\cos k_w z - \theta \\ -\psi \end{pmatrix}\ . \tag{1.7}$$

The purpose of this paper is to evaluate the integral appearing in Eq. (1.1) and to exhibit its behavior, not to justify its derivation further. For brevity the constant factor in the denominator of the left hand side will be suppressed. This makes the implicit assumption, standard in the field, though often not entirely valid, that the distance $\mathcal{R}$ to the observation point is large compared to the undulator length. It has also been assumed that the transverse displacement of the electron in the undulator is small compared to the transverse displacement of the observation point.

Following Kim[1] (though not in detail) as well as (and more closely) Als-Nielsen and McMorrow,[4] to use Eq. (1.6) it is useful to re-arrange it so that the linear term is the same as the arguments of the trigonometric factors. Toward that end we introduce

$$\omega_1(\vartheta) = \frac{2\gamma^2}{1 + K^2/2 + \gamma^2\vartheta^2}\,ck_w\ ; \tag{1.8}$$

† Later, while evaluating Eq. (1.1) it will not be legitimate to cavalierly drop terms like ϑ^2, but that will be because they occur in the exponent.

$\omega_1(\vartheta)$ is the $n = 1$ undulator resonance frequency *at the particular angle* ϑ. This anticipates a result that, logically speaking, will be an *output* from the calculation, but is presumably well known in advance. In particular, the formula includes the well known result that in the limit of "ideal" undulator action ($K << 1$), at the fundamental ($n = 1$) resonance, the peak wavelength (in the forward direction) is given by $\lambda_w/(2\gamma^2)$. The general resonance formula is

$$\omega_n\left(\vartheta\right) = n\,\omega_1\left(\vartheta\right) \ . \tag{1.9}$$

At given angle ϑ this gives the central frequency of the narrow band of frequencies corresponding to the n'th instance of constructive interference from successive poles. This nearly one-to-one relation between ϑ and ω at given n must be remembered while inspecting graphical representations of the radiation.

Other variables to be used are

$$\phi_t = \omega_1\left(\vartheta\right)\, t, \quad \text{and} \quad \phi_z = k_w z \approx k_w c t_r \ . \tag{1.10}$$

The newly introduced quantity ϕ_t is the observation time expressed as a phase angle, where the phase is referred to frequency $\omega_1(\vartheta)$. Then Eq. (1.6) becomes†

$$\begin{aligned} \phi_t &= \phi_z - \frac{2\gamma\theta K}{1 + K^2/2 + \gamma^2\vartheta^2}\,\sin\phi_z + \frac{K^2/4}{1 + K^2/2 + \gamma^2\vartheta^2}\,\sin 2\phi_z \\ &\equiv \phi_z + p\,\sin\phi_z + q\,\sin 2\phi_z \ . \end{aligned} \tag{1.11}$$

Substituting into Eq. (1.1), changing integration variable from t_r to ϕ_z, and temporarily taking N_w to be odd‡, yields

$$\widetilde{\mathbf{E}}\left(\omega;\theta,\psi\right) = \frac{i\omega}{\sqrt{2\pi}}\int_{-N_w\pi}^{N_w\pi} \exp\left(i\,\frac{\omega}{\omega_1\left(\vartheta\right)}\,\left(\phi_z + p\,\sin\phi_z + q\,\sin 2\phi_z\right)\right)\begin{pmatrix}\Theta\,\cos\phi_z - \theta \\ -\psi\end{pmatrix}\frac{d\phi_z}{k_w c}\,, \tag{1.12}$$

† Our p and q need to be multiplied by $\mp\omega/\omega_1(\vartheta)$ respectively to be the same as Kim's p and q. Kim's Eq.(4.23) has a typographical error that is corrected in later formulas—his K should be replaced by the equivalent of our Θ.

‡ If the integration range is taken to be from $-\pi$ to $(2N_w - 1)\pi$ (with N_w either even or odd) the summation in the following equation (1.13) is just multiplied by a factor $\exp(i\pi(N_w - 1)\omega/\omega_1)$, which has magnitude 1. Because the overall phase depends on choice of origin it is in any case arbitrary, and drops out when the (measureable) square of absolute value is taken. Hence N_w can be taken either even or odd in subsequent formulas. In principle there could be interference between contributions of the same frequency from difference undulator resonances, in which case the phase could be meaningful.

We can now exploit the periodic nature of the exponent and integrand to represent the integral as a sum;

$$\widetilde{\mathbf{E}}\left(\omega;\theta,\psi\right) = \frac{i}{\sqrt{2\pi}}\,\frac{\omega}{k_w c}\left(\sum_{j=-(N_w-1)/2}^{(N_w-1)/2} \exp\left(i\frac{\omega}{\omega_1\left(\vartheta\right)}\,2\pi\, j\right)\right)$$
$$\times\int_{-\pi}^{\pi} \exp\left(i\frac{\omega}{\omega_1\left(\vartheta\right)}\,\left(\phi_z + p\,\sin\phi_z + q\,\sin 2\phi_z\right)\right)\begin{pmatrix}\Theta\,\cos\phi_z - \theta \\ -\psi\end{pmatrix}\,d\phi_z \tag{1.13}$$

This is the main formula to be evaluated. Since the integral is independent of N_w, one has obtained a useful factorization into a "phasor sum" part (which can be readily summed)

$$\sum_{j=-(N_w-1)/2}^{(N_w-1)/2} \exp\left(2\pi i\frac{\omega}{\omega_1\left(\vartheta\right)}\,j\right) = \frac{\exp\left(-\pi i\,\frac{\omega}{\omega_1(\vartheta)}\,\left(N_w-1\right)\right) - \exp\left(\pi i\,\frac{\omega}{\omega_1(\vartheta)}\,\left(N_w+1\right)\right)}{1-\exp\left(2\pi i\,\frac{\omega}{\omega_1(\vartheta)}\right)}$$
$$= \frac{\sin\left(N_w\pi\omega/\omega_1\left(\vartheta\right)\right)}{\sin\left(\pi\omega/\omega_1\left(\vartheta\right)\right)} \tag{1.14}$$

and the "single period amplitude"

$$i\sqrt{\frac{2}{\pi}}\,\frac{\omega}{k_w c}\int_0^{\pi}\cos\left(i\frac{\omega}{\omega_1\left(\vartheta\right)}\,\left(\phi_z + p\,\sin\phi_z + q\,\sin 2\phi_z\right)\right)\begin{pmatrix}\Theta\,\cos\phi_z - \theta \\ -\psi\end{pmatrix}\,d\phi_z\ . \tag{1.15}$$

Results obtained by evaluating this integral numerically will be said to be "exact" for purposes of this paper, even though some approximations have entered its derivation.

2. Expansion-About-Resonance Approximation

It is integral (1.15) that is to be evaluated both numerically and analytically in the remainder of the paper. But before doing so, to initiate qualitative discussion, and then to concentrate on the forward peak, especially for $N_w >> 1$, let us introduce "fractional frequency" ν and "fractional frequency offset" $\Delta\nu$;

$$\nu = \frac{1}{n}\,\frac{\omega}{\omega_1\left(\vartheta\right)} = 1+\Delta\nu\ . \tag{2.1}$$

Exactly on resonance (i.e. at integer values of n) the value of the phasor sum is

$$\sum\Big|_{\Delta\nu=0} = \frac{d/d\Delta\nu\,\sin\left(N_w\pi n\left(1+\Delta\nu\right)\right)}{d/d\Delta\nu\,\sin\left(\pi n\left(1+\Delta\nu\right)\right)}\Big|_{\Delta\nu=0} = N_w\,\left(-1\right)^{(N_w-1)n} = N_w\ . \tag{2.2}$$

(The last step continues to assume N_w odd.) The phasor sum factor is therefore given by

$$\sum = N_w\,\frac{\sin\left(N_w\pi n\Delta\nu\right)}{N_w\pi n\Delta\nu} \equiv N_w\,\mathrm{sinc}\left(N_w\pi n\Delta\nu\right),\quad n=0,1,2,3,\dots\ . \tag{2.3}$$

Since this factor is approximately equivalent to a comb of Dirac delta functions, the factor it multiplies needs only to be evaluated on-resonance. One therefore makes the replacement $\omega/\omega_1(\vartheta) \rightarrow n$ in the integrand of Eq. (1.15), yielding

$$\widetilde{\mathbf{E}}\left(\omega;\theta,\psi\right) \approx \sum_{n=1}^{\infty} \widetilde{\mathbf{E}}_n\left(\theta,\psi\right)\, nN_w \,\mathrm{sinc}\left(N_w\pi\left(\frac{\omega}{\omega_1\left(\vartheta\right)} - n\right)\right)\ , \tag{2.4}$$

where

$$\widetilde{\mathbf{E}}_n\left(\theta,\psi\right) = i\sqrt{\frac{2}{\pi}}\,\frac{2\gamma^2}{1+K^2/2+\gamma^2\vartheta^2}\times$$
$$\int_0^\pi \cos\left(n\left(\phi_z - \frac{2\gamma\theta K\,\sin\phi_z}{1+K^2/2+\gamma^2\vartheta^2} + \frac{\left(K^2/4\right)\,\sin 2\phi_z}{1+K^2/2+\gamma^2\vartheta^2}\right)\right)\begin{pmatrix}\Theta\,\cos\phi_z - \theta\\ -\psi\end{pmatrix} d\phi_z\ . \tag{2.5}$$

In this form there appear to be extrema at all integer values of n. But this is somewhat misleading. For most practical purposes one is interested in the radiation almost in the forward direction, $\theta = \psi = 0$. This leaves only the x-component $\widetilde{E}_{x,n}(0,0)$), the term proportional to Θ, in which case the integral vanishes for all even values of n. This is because of destructive interference between the positive-going and negative-going portions of a single wiggler period; it is easiest to see this in the limit of long wavelengths ($n = 0$). These comments are the basis of the probably overly-glib statement "undulator radiation consists of odd harmonics" which is valid only in this restricted sense. For $\theta = 0$ one has $p = 0$ in Eq. (2.5), the dominant (upper) integral can be evaluated analytically for odd n;

$$\widetilde{\mathbf{E}}_n\left(0,\psi\right) = i\sqrt{\frac{\pi}{2}}\,\frac{n\omega_1\left(\vartheta\right)}{k_w c}\,\frac{K}{\gamma}\,\left(J_{\frac{n+1}{2}}\left(-nq\right) + J_{\frac{n-1}{2}}\left(-nq\right)\right),\quad n = 1,3,5,\ldots \tag{2.6}$$

This is Eq. (4.45) of Kim. For many purposes this equation, taken with Eq. (2.4), gives an adequate description of the undulator radiation. We will see though that, as well as being restricted to odd n, and giving only the x component at that, it misses entirely the bizarre dependence on θ already present at extremely small angles (in the range $0 < \theta < 1/(n\gamma)$) and even with $N_w = 1$.

In spite of these defects, since Eq. (2.6) is valid in the center of the region of greatest importance for the practical use of synchrotron radiation, it is appropriate to investigate its predictions. There is an inevitable trade-off in which the undulator beam frequency $\omega_n(0)$ and intensity $|\mathbf{E}|^2$ are made as high as possible consistent with the machine energy

γ being as small as possible and undulator wave length λ_w as large as possible (so the undulator gap height can be as large as possible). For "cleaner" operation one prefers both the undulator parameter K and the harmonic number n to be as low as possible. (At least until accelerator physics issues intrude, the bigger the better for N_w.) The first formula governing this trade-off is Eq. (1.9);

$$\frac{\omega_n(0)}{ck_w 2\gamma^2} = \frac{n}{1+K^2/2} \,, \tag{2.7}$$

by which the resonant frequency can be increased by increasing n but is unavoidably decreased by increasing K. The second key result, from Eqs. (1.11) and (2.6), is

$$\frac{|\mathbf{E}_n|^2(0)}{\gamma^2} = \frac{\pi}{2}\left(\frac{2K\,n}{1+K^2/2}\right)^2\left(J_{\frac{n+1}{2}}\left(\frac{-nK^2/4}{1+K^2/2}\right) + J_{\frac{n-1}{2}}\left(\frac{-nK^2/4}{1+K^2/2}\right)\right)^2 \,, \tag{2.8}$$

These formulas are evaluated for ranges of n and K, and the results exhibited numerically in the following table and graphically in Fig. 2.1. In each case in the table the upper number is given by Eq. (2.8) and the lower is given by Eq. (2.7).

n\K	0	.2	.4	.6	.8	1.0	1.2	1.4	1.6	1.8	2.0	2.4	2.6	2.8	3.0
1	0.	.24	.83	1.5	2.0	2.3	2.4	2.3	2.2	2.0	1.8	1.6	1.5	1.3	1.2
	1.	.98	.93	.85	.76	.67	.58	.51	.44	.38	.33	.29	.26	.23	.20
3	0.	.46e-3	.023	.17	.55	1.1	1.7	2.2	2.5	2.7	2.7	2.6	2.4	2.3	2.1
	3.	2.9	2.8	2.5	2.3	2.0	1.7	1.5	1.3	1.1	1.0	.88	.77	.68	.61
5	0.	.54e-6	.37e-3	.011	.092	.35	.80	1.4	1.9	2.3	2.6	2.7	2.7	2.7	2.5
	5.	4.9	4.6	4.2	3.8	3.3	2.9	2.5	2.2	1.9	1.7	1.5	1.3	1.1	1.0
7	0.	.53e-9	.52e-5	.67e-3	.013	.091	.32	.74	1.3	1.8	2.2	2.5	2.7	2.7	2.7
	7.	6.9	6.5	5.9	5.3	4.7	4.1	3.5	3.1	2.7	2.3	2.0	1.8	1.6	1.4
9	0.	.48e-12	.67e-7	.36e-4	.0018	.022	.12	.37	.79	1.3	1.8	2.2	2.5	2.7	2.8
	9.	8.8	8.3	7.6	6.8	6.0	5.2	4.5	3.9	3.4	3.0	2.6	2.3	2.1	1.8
11	0.	.41e-15	.82e-9	.19e-5	.23e-3	.0053	.043	.18	.47	.89	1.4	1.9	2.2	2.5	2.7
	11.	11.	10.	9.3	8.3	7.3	6.4	5.6	4.8	4.2	3.7	3.2	2.8	2.5	2.2

An example may help to clarify this data. Consider the points $(n, K, \mathrm{int.}, \mathrm{freq.}) = (1, 0.2, 0.24, 0.98), (3, 0.6, 0.17, 2.5), (5, 0.8, 0.092, 3.8), (7, 1.0, 0.091, 4.7), (9, 1.2, 0.12, 5.2)$. These points have comparable intensities but, by increasing n and K together, it is possible to increase the beam frequency from 0.98 to 5.2 (in units of $ck_w 2\gamma^2$.) Being proportional to K^2, the total radiated beam power increases by a considerably greater factor of 36 over this range. The beam is therefore much "cleaner" for low n values than for high; that is, the ratio of useful to useless power is higher. Calculations like this are useful in fixing the major storage ring and undulator parameters to achieve high brilliance.

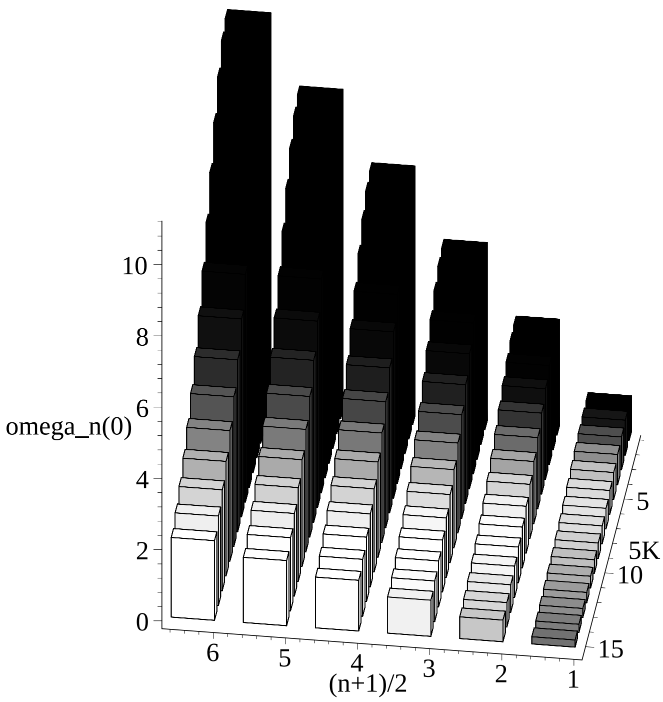

Figure 2.1: Histograms illustrating the dependence of undulator frequency (indicated by tower height) and intensity on resonance (indicated by tower grayscale) on undulator parameter $0 < K < 3.0$ and resonance order $n = 1, 3, 5, 7, 9, 11$. The grayscale is the same as in Fig. 3.1 and is normalized to 1 (white) in the lower left hand corner. Black regions have negligible flux.

3. Some Undulator Distributions

This section contains coarse undulator distributions obtained by numerical evaluation of Eq. (1.15) for (moderately low) values of $n = 3$ and $n = 5$. Since the *sinc* factor is not included for these plots, they exhibit the "modulating profile" that must be multiplied by a "delta-function-like" *sinc*. For given direction (θ, ψ) (and hence given ϑ) the effect is to give only photons in a narrow band of frequencies close to $\omega_n(\vartheta)$ as given by Eq. (1.9). The angular intensity pattern is proportional to $|\widetilde{E}_{n,x}|^2(\theta, \psi)$ which is exhibited for $K = 1.5$, $n = 3, 5$, in Fig. 3.1 and Fig. 3.2. Each histogram tower represents both $|\widetilde{E}_{3,x}|^2_{K=1.5}(\theta, \psi)$

and the ratio $\omega(\theta, \psi)/\omega_3(0)$. The intensity is represented by the height of the tower and the photon energy by its grayscale value.

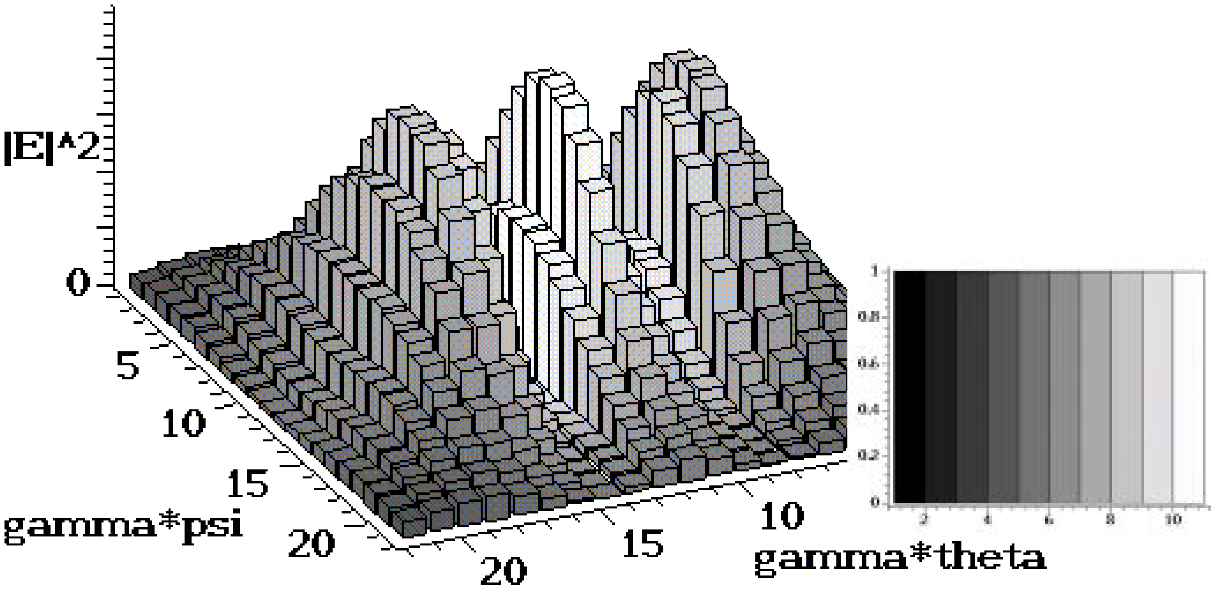

Figure 3.1: Histogram representation of undulator radiation: the height of each bin gives the value of $|\widetilde{E}_{3,x}|^2_{K=1.5}(\theta, \psi)$, as given by Eq. (2.5) at the appropriate value of $(\gamma\theta, \gamma\psi)$. Since the photon frequency ω is known as a function of the same independent-variable pair (θ, ψ) (Eq. (1.9)), it can be exhibited as a ratio $\omega/\omega_3(0)$ which is coded by the grayscale shading. The forward direction is marked by the highest tower which has $\omega/\omega_3(0) = 1$ and is therefore pure white. 'gamtheta' and 'gampsi' stand for $\gamma\theta$ and $\gamma\psi$. The bin widths are $\Delta\theta = \Delta\psi = 0.15/\gamma$. The vertical scale is not shown, but it extends uniformly from 0 to 2.5×10^8. This data is independent of N_w.

The bin widths are $\gamma\Delta\theta = \gamma\Delta\psi = 0.15$. A detector having these acceptances and centered, say, at the origin, would count only photons of frequency $\omega = \omega_3(0)$ (which makes the tower pure white.) Assuming the detector accepts all photons close to this energy (so the sinc-factor can be treated as a δ-function) the rate can be read off from the vertical axis, but still needs multiplication by the factor nN_w appearing in Eq. (2.4) and by the factor $\Delta\theta\,\Delta\psi$. If the detector's fractional frequency acceptance is small compared to $1/N_w$ (as is common) it is necessary to treat the sinc-factor dependency more carefully.

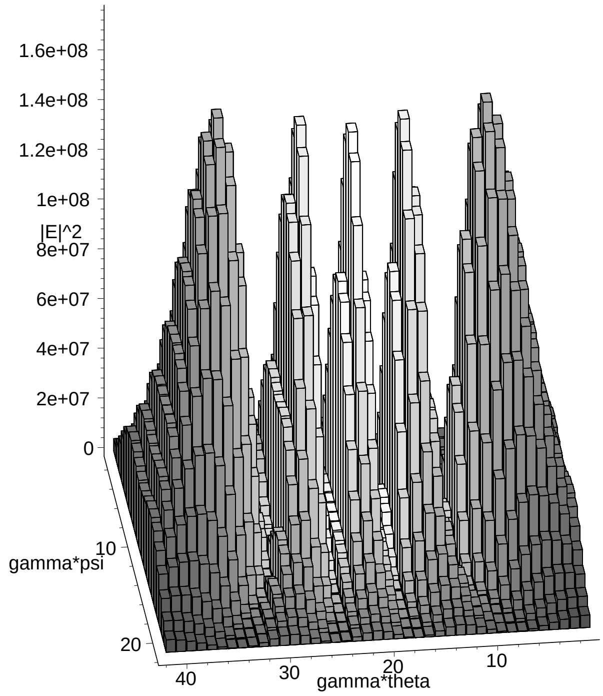

Figure 3.2: Same as previous figure except now $n = 5$ and bin spacings are $2\Delta\theta = \Delta\psi = 0.15/\gamma$. Again the unique pure white tower is in the forward direction.

The structure of Fig. 3.2 can be understood qualitatively. The angular separation $\Delta\theta$ of fringe maxima is approximately $5\times 0.075/\gamma = 0.375/\gamma$. The factor $\sin k_w z$ advances from 0 to 1 between north and south magnet poles, so the second term on the rhs of Eq. (1.6) gives a phase advance (with $n = 5$, $K \equiv \Theta\gamma = 1.5$) equal to $5 \times 2\gamma \times 1.5 \times 0.375/\gamma \approx 2\pi$. This is why angular fringes are visible even with $N_w = 1$. With $N_w >> 1$ and the sinc-factor included, the peaks would be much narrower but the grayscale values would be unchanged.

There appears to be no universally accepted distinction between "undulator operation" and "wiggler operation", though $K = 1$ is commonly quoted as the dividing line. Here is another suggestion. The spacing of the fringe structure in the θ direction (visible in Fig. 3.2) decreases as n increases. This fringe structure is independent of N_w. This suggests the definition: *For undulator operation the fringe structure is large compared to the experimental resolution. For wiggler operation the fringe structure is not resolved by the* *detection apparatus.* If this fringe structure is averaged out there seems to be no essential distinction between undulator and wiggler operation.

4. Approximation of the Integrals By Special Functions

To describe undulator radiation conveniently at general angles and frequencies what is required is a generalization of Eq. (2.6). Apart from the facts that p has been set to zero in deriving that equation, and that *even* values of n give fractional Bessel indices, the fact that Bessel functions are singular as functions of their indices complicates the task.

The integrand in Eq. (1.15) can be Taylor expanded in terms of the (small) variable θ

$$\begin{aligned}\cos\left(\eta\phi+\eta p\,\sin\phi+\eta q\,\sin 2\phi\right) =\; &\cos\left(\eta\phi+\eta q\,\sin 2\phi\right)\left(1-\frac{\eta^2p^2}{4}+\frac{\eta^2p^2}{4}\,\cos 2\phi+\ldots\right)\\ -\; &\sin\left(\eta\phi+\eta q\,\sin 2\phi\right)\left(\eta p\,\sin\phi+\ldots\right),\end{aligned} \tag{4.1}$$

and further terms can be derived easily. Here, motivated by Eq. (2.4), we have generalized the meaning of variable n and replaced it by the symbol η by making the substitution

$$\frac{\omega}{\omega_1\left(\vartheta\right)}=\eta\ . \tag{4.2}$$

This means that η is allowed to lie anywhere in the range $0<\eta<\infty$ and, in particular, to not necessarily be an integer. Nevertheless, especially for large N_w, the *sinc* factor suppresses the complete expression when η is not close to an integer, so η can be thought of as being "close" to a particular integer n.

Using abbreviation $\mathcal{C}\equiv\cos(\eta\phi+\eta q\,\sin 2\phi)$ we define standard integrals

$$I_{C0}=\int_0^{\pi}\mathcal{C}\,d\phi,\quad I_{C1}=\int_0^{\pi}\mathcal{C}\,\cos\phi\,d\phi,\quad I_{C2}=\int_0^{\pi}\mathcal{C}\,\cos 2\phi\,d\phi\ , \tag{4.3}$$

and integrals $I_{S1},I_{S2},\ldots$, are defined similarly, but with $\mathcal{C}$ replaced by $\mathcal{S}\equiv\sin(\eta\phi+\eta q\,\sin 2\phi)$. The required integral is

$$\begin{aligned}&\int_0^{\pi}d\phi\,\cos\left(\eta\phi+\eta p\,\sin\phi+\eta q\,\sin 2\phi\right)\left[\begin{pmatrix}\Theta\\0\end{pmatrix}\cos\phi+\begin{pmatrix}-\theta\\-\psi\end{pmatrix}\right]\\ &\quad=\begin{pmatrix}\Theta\left(1-\eta^2p^2/8\right)\\0\end{pmatrix}I_{C1}+\begin{pmatrix}\Theta\,\eta^2p^2/8\\0\end{pmatrix}I_{C3}+\begin{pmatrix}-\eta p\Theta/2\\0\end{pmatrix}I_{S2}\\ &\quad+\begin{pmatrix}-\theta\left(1-\eta^2p^2/4\right)\\-\psi\left(1-\eta^2p^2/4\right)\end{pmatrix}I_{C0}+\begin{pmatrix}-\theta\eta^2p^2/4\\-\psi\eta^2p^2/4\end{pmatrix}I_{C2}+\begin{pmatrix}\eta p\theta\\\eta p\psi\end{pmatrix}I_{S1}+\ldots\ .\end{aligned} \tag{4.4}$$

I_{C1} was evaluated for odd integer n in obtaining Eq. (2.6), but it, and the other integrals, can now be expressed for arbitrary η and for positive integers j as

$$\begin{aligned} I_{Cj} &= \frac{1}{4}\int_0^{2\pi} \cos\left(\frac{\eta-j}{2}\xi + \eta q\,\sin\xi\right)\,d\xi + \frac{1}{4}\int_0^{2\pi} \cos\left(\frac{\eta+j}{2}\xi + \eta q\,\sin\xi\right)\,d\xi \\ I_{Sj} &= \int_0^{\pi} \sin\left(\eta\phi + \eta q\,\sin 2\phi\right)\,\sin j\phi\,d\xi \\ &= \frac{1}{4}\int_0^{2\pi} \cos\left(\frac{\eta-j}{2}\xi + \eta q\,\sin\xi\right)\,d\xi - \frac{1}{4}\int_0^{2\pi} \cos\left(\frac{\eta+j}{2}\xi + \eta q\,\sin\xi\right)\,d\xi \end{aligned} \tag{4.5}$$

All these integrals can be expressed in terms of the functions

$$\begin{aligned} \pi\,\mathbf{J}_\mu &= \int_0^{\pi} \cos\left(\mu\,\theta - z\,\sin\theta\right)\,d\theta \\ \pi\,\mathbf{E}_\mu &= \int_0^{\pi} \sin\left(\mu\,\theta - z\,\sin\theta\right)\,d\theta \end{aligned} \tag{4.6}$$

where $\mathbf{J}_i$ is known as an "Anger" function and $\mathbf{E}_i$ as a "Weber" function. The standard reference is Watson[5]; this formula is on page 308. These definitions are valid for general values of μ. Both functions are known to MAPLE which calculates them rapidly. Bisecting the range, and replacing θ by $2\pi - \theta$ in the second integral, Watson gives the formula

$$\begin{aligned} \int_0^{2\pi} \cos\left(\mu\,\theta - z\,\sin\theta\right)\,d\theta &= \int_0^{\pi} \left(\cos\left(\mu\,\theta - z\,\sin\theta\right) + \cos\left(2\mu\pi - \mu\theta + z\sin\theta\right)\right)\,d\theta \\ &= 2\pi\,\cos^2\mu\pi\;\mathbf{J}_\mu\left(z\right) + \pi\,\sin 2\mu\pi\;\mathbf{E}_\mu\left(z\right)\;. \end{aligned} \tag{4.7}$$

In terms of these functions the required integrals are

$$\begin{aligned} I_{Cj} = &\frac{\pi}{2}\cos^2\left(\frac{\eta-j}{2}\pi\right)\,\mathbf{J}_{\frac{\eta-j}{2}}\left(-\eta q\right) + \frac{\pi}{4}\sin\left(\left(\eta-j\right)\pi\right)\,\mathbf{E}_{\frac{\eta-j}{2}}\left(-\eta q\right)\;, \\ &+\frac{\pi}{2}\cos^2\left(\frac{\eta+j}{2}\pi\right)\,\mathbf{J}_{\frac{\eta+j}{2}}\left(-\eta q\right) + \frac{\pi}{4}\sin\left(\left(\eta+j\right)\pi\right)\,\mathbf{E}_{\frac{\eta+j}{2}}\left(-\eta q\right)\;, \\ I_{Sj} = &\frac{\pi}{2}\cos^2\left(\frac{\eta-j}{2}\pi\right)\,\mathbf{J}_{\frac{\eta-j}{2}}\left(-\eta q\right) + \frac{\pi}{4}\sin\left(\left(\eta-j\right)\pi\right)\,\mathbf{E}_{\frac{\eta-j}{2}}\left(-\eta q\right)\;, \\ &-\frac{\pi}{2}\cos^2\left(\frac{\eta+j}{2}\pi\right)\,\mathbf{J}_{\frac{\eta+j}{2}}\left(-\eta q\right) - \frac{\pi}{4}\sin\left(\left(\eta+j\right)\pi\right)\,\mathbf{E}_{\frac{\eta+j}{2}}\left(-\eta q\right)\;. \end{aligned} \tag{4.8}$$

5. Practical Evaluation of the Series

The Taylor expansion of Eq. (4.4) can be spelled out in general as follows:

$$
\begin{aligned}
f(m,j) &= \frac{\mathrm{binomial}\,(m,(m-j)/2)}{m!\,2^{(m-1)}} \\
a(\eta,j) &= (-1)^{j/2}\sum_{0}^{i_{\max}}(-1)^{i}\,(\eta p)^{2i}\,f(2i,j)\,,\quad j=0,2,4,\dots \\
a_0(\eta) &= a(\eta,0)/2, \\
b(\eta,j) &= (-1)^{(j-1)/2}\sum_{0}^{i_{\max}}(-1)^{i}\,(\eta p)^{(2i+1)}\,f(2i+1,j)\,,\quad j=1,3,5,\dots \\
\gamma\widetilde{E}_x(\eta) &= \frac{K}{2}\left(2a_0(\eta)+a(\eta,2)\right)I_{C,1} \\
&\quad+\frac{K}{2}\sum_{i'=1}^{i_{\max}-1}\left(a\left(\eta,2i'\right)+a\left(\eta,2i'+2\right)\right)I_{C,2i'+1}+\frac{K}{2}\,a\left(\eta,2i_{\max}\right)I_{C,2i_{\max}+1} \\
&\quad-\frac{K}{2}\sum_{i'=0}^{i_{\max}-1}\left(b\left(\eta,2i'+1\right)+b\left(\eta,2i'+3\right)\right)I_{S,2i'+2}-\frac{K}{2}\,b\left(\eta,2i_{\max}+1\right)I_{S,2i_{\max}+2} \\
&\quad-\gamma\theta\left(a_0(\eta)\,I_{C,0}+\sum_{i'=1}^{i_{\max}}a\left(\eta,2i'\right)I_{C,2i'}-\sum_{i'=0}^{i_{\max}}b\left(\eta,2i'+1\right)I_{S,2i'+1}\right) \\
\gamma\widetilde{E}_y(\eta) &= -\gamma\psi\left(a_0(\eta)\,I_{C,0}+\sum_{i'=1}^{i_{\max}}a\left(\eta,2i'\right)I_{C,2i'}-\sum_{i'=0}^{i_{\max}}b\left(\eta,2i'+1\right)I_{S,2i'+1}\right);
\end{aligned}
\tag{5.1}
$$

these expressions still need to be multiplied by the factor

$$
i\sqrt{\frac{2}{\pi}}\,\frac{\omega}{k_w c}\,\frac{\sin N_w\pi\eta}{\sin\pi\eta}\;; \tag{5.2}
$$

this factor (except for the i) is included for the following graphs. The maximum power of p retained in the expansion is $2i_{\max}+1$. For constant accuracy $i_{\max}$ has to increase with increasing $\gamma\vartheta$. At fixed K the ring structure depends only on $\gamma\vartheta$. Because an oscillatory function is being fit by a power series, the number of cycles fit is probably proportional to the highest power retained. From the example we have studied most carefully ($K=1.35$) a suggested rule of thumb is to choose $i_{\max}$ to be about four (or more) times the number of rings to be faithfully calculated, but this should be investigated in each case. The following three pairs of graphs illustrate these comments.

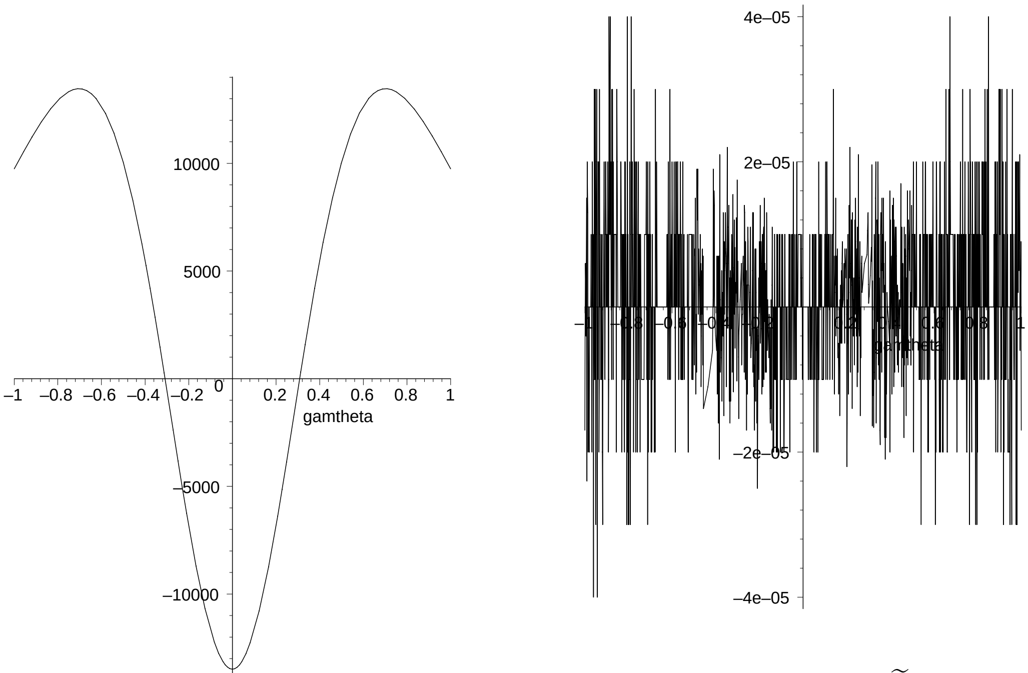

Figure 5.1: The left graph shows (superimposed) the values of $|\widetilde{\mathbf{E}}(\gamma\theta, \gamma\psi = 0.3, n = 3)|^2$ as given by integral (1.13) evaluated numerically and by using the method of section 5; $i_{\max} = 14$

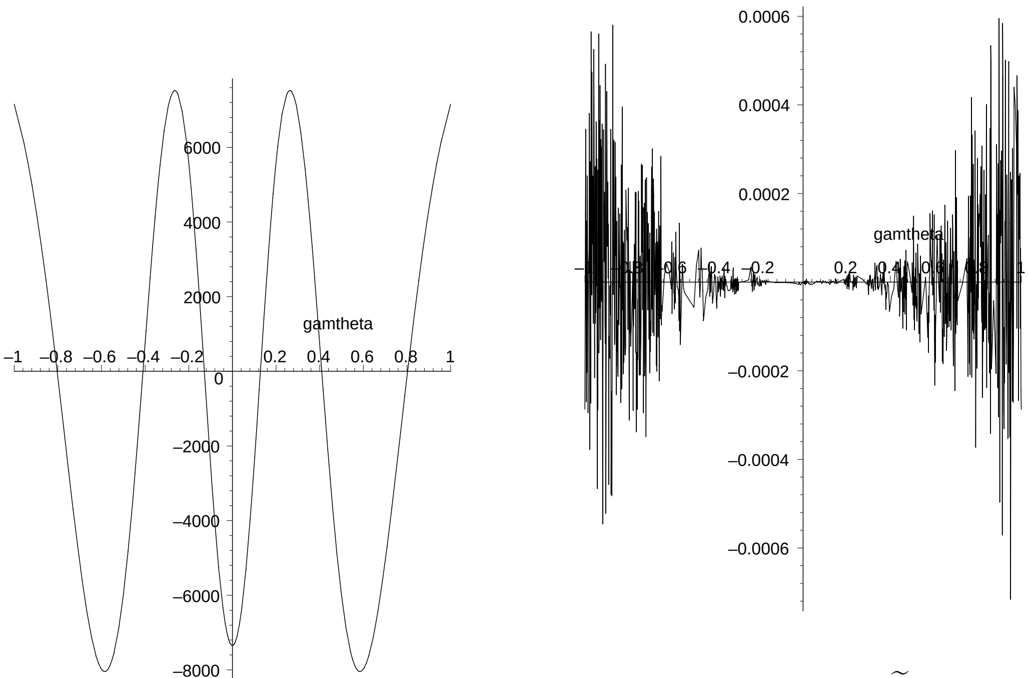

Figure 5.2: The left graph shows (superimposed) the values of $|\widetilde{\mathbf{E}}(\gamma\theta, \gamma\psi = -0.2, n = 7)|^2$ as given by integral (1.13) evaluated numerically and by using the method of section 5; $i_{\max} = 14$

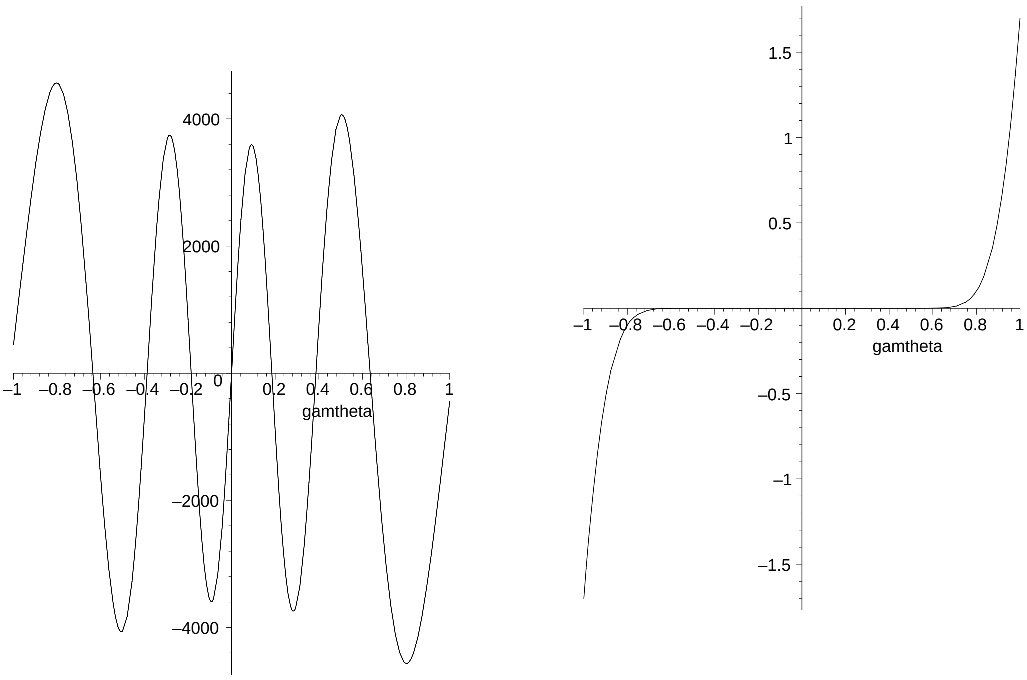

Figure 5.3: The left graph shows (superimposed) the values of $|\widetilde{\mathbf{E}}(\gamma\theta, \gamma\psi = 0.2, n = 10)|^2$ as given by integral (1.13) evaluated numerically and by using the method of section 5; $i_{\max} = 14$.

The fractional accuracy is excellent over the full range $-1/\gamma < \theta < 1/\gamma$ which includes essentially all the radiation. To obtain excellent accuracy in the experimentally relevant region of the central peak it is sufficient to use only the terms exhibited explicitly in Eq. (4.4).

Since θ, but not ψ, has been assumed small in deriving Eq. (4.4), its region of validity should be a narrow band centered on the ψ-axis. From Fig. 3.1 and Fig. 3.2 one knows that the radiation pattern is made up of parallel valleys separated by long mountains that are aligned with the ψ-axis. Since the variation with θ (at fixed ψ) is roughly sinusoidal (squared) one cannot expect a power series truncated to the terms shown explicitly in Eq. (4.4) to remain accurate outside the central three mountains. Nevertheless this truncated (and hence quite simple) form should be useful in practice because it it is the central mountain that is mainly used in most applications of undulator radiation.

6. Post-Monochrometer Profile

The beam from the undulator is typically passed through a monochrometer which passes only frequencies in a narrow band centered at, say,

$$\omega_{\mathrm{mono.}} = n_{\mathrm{mono.}}\, \omega_1\left(0\right), \tag{6.1}$$

where $n_{\mathrm{mono.}}$ is set to an integer or, typically, slightly below an integer. (For the example to be worked out shortly $n_{\mathrm{mono.}} = 7.0$.) Substituting this into Eq. (4.2) yields

$$\eta\left(\vartheta\right) = n_{\mathrm{mono.}} \frac{1 + K^2/2 + \gamma^2\vartheta^2}{1 + K^2/2} \tag{6.2}$$

as the appropriate parameter at which integral (4.4) is to be evaluated.† For large N_w we know that the phasor factor will suppress the field unless η is close to an integer; call it $n_{\mathrm{harm.}}$ where

$$n_{\mathrm{mono.}} \leq n_{\mathrm{harm.}} \leq n_{\mathrm{max.}}, \tag{6.3}$$

where $n_{\mathrm{max.}}$ is the highest undulator harmonic that is kinematically possible or some arbitrarily chosen maximum value of interest. The analysis would be simplest for $n_{\mathrm{mono.}} = n_{\mathrm{max.}}$ but, in practice, it may be desirable to center the monochrometer on an undulator resonance lower than the maximum possible. (For the example to be worked out shortly $n_{\mathrm{max.}} = 10$.) When this is done the harmonics for which $n_{\mathrm{harm.}} > n_{\mathrm{mono.}}$ yield circular ring profiles centered on the undulator axis, at angle $\vartheta_{\mathrm{harm.}}$ given by solving Eq. (6.2) to obtain

$$\gamma\vartheta_{\mathrm{harm.}} = \sqrt{\left(1 + \frac{K^2}{2}\right)\frac{n_{\mathrm{harm.}} - n_{\mathrm{mono.}}}{n_{\mathrm{mono.}}}}\ . \tag{6.4}$$

The convergence of series (4.4) is worst for $n_{\mathrm{harm.}} = n_{\mathrm{max.}}$. To save computer time it is sensible to calculate only at points for which the phasor factor is not negligibly small. The larger N_w is, the slimmer are the rings in which there is any appreciable response. For example in generating Fig. 6.1 we have taken $\Delta n_{\mathrm{harm.}} = \pm 1/N_w$ as the range over which the phasor factor is not negligible. This suppresses secondary diffraction rings having intensities in the several percent range.

---

† Note the surprising result that the argument of the Bessel-like functions entering the post-monochrometer profile, namely $\eta(\vartheta)\, q = n_{\mathrm{mono.}}(K^2/4)/(1+K^2/2)$, is independent of ϑ and hence of emission direction. This gives no important simplification because the indices depend on direction.

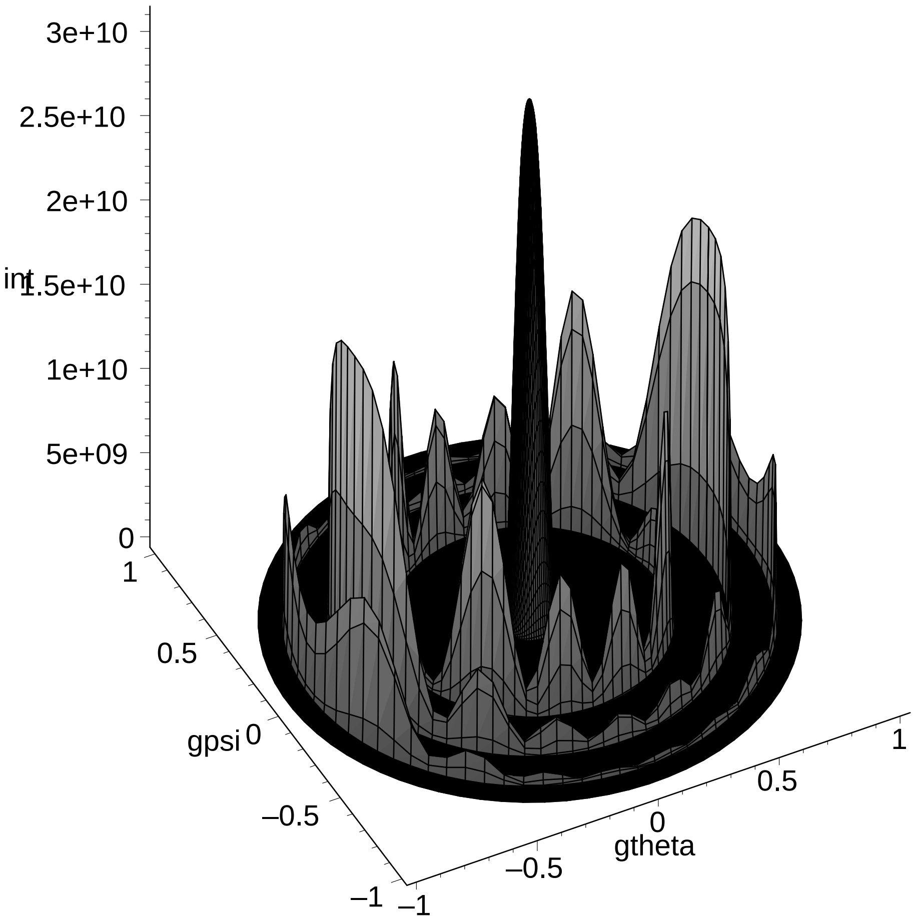

Figure 6.1: Spectrum for published ESRF configuration as recalculated using Eq. (4.4). Physical parameters were $E = 6\,\text{GeV}$, $N_w = 20$, $\lambda_w = 46\,\text{mm}$, $E_\gamma = 27\,\text{keV}$. Calculational parameters are $N_w = 19$, $i_{\max} = 14$, $n_{\text{mono.}} = 7$. This result can be directly compared with another calculation: www.esrf.fr/machine/support/ids/Public/CentralCone/CentralCone.html

References

1. K. Kim, *Characteristics of Synchrotron Radiation*, in *Physics of Particle Accelerators*, M. Month and M. Dienes, editors, AIP 184, 1988, (2.22).
2. J. D. Jackson, *Classical Electrodynamics*, John Wiley, 1975, (14.67).
3. R. P. Walker, *Insertion Devices: Undulators and Wigglers,* in CERN 98-04, ??.
4. J. Als-Nielsen and D. McMorrow, *Elements of Modern X-Ray Physics*, John Wiley, 2001.
5. G. N. Watson, *A Treatise on the Theory of Bessel Functions*, 2nd Ed. Cambridge, 1958.